

Numerical analysis of the microclimate conditions around a new telescope in La Palma, Spain

D. Pérez

CIMNE, Spain

G. Houzeaux

Universitat Politècnica de Catalunya and CIMNE, Spain

J. Cipriano

CIMNE, Spain

ABSTRACT

This work aims at applying a numerical analysis methodology, based on CFD techniques, to evaluate the effect of the wind and the temperature over the quality vision of a new telescope in La Palma (Spain). This island constitutes one of the best places in the world to carry out astronomy experiments. However, small variations in the climate conditions, together with the particle dispersion, drastically affect the selection of the best place where this building may be installed. In this work, the surrounding flow pattern and the turbulence distribution of the two possible places will be evaluated and analyzed. The numerical simulation will include a discretization of La Palma island, statistic analysis of the wind variation and a detailed analysis of the wind turbulences due to the terrain obstacles and other telescope buildings.

1. INTRODUCTION

We present in this work a numerical strategy to solve external airflows around telescope buildings. The computational domain is large enough to ensure that its boundaries are placed sufficiently far from the calculation domain (island/building). In this way the calculated flow pattern around the computational domain will not be affected by the external boundaries of the computational domain (Scaperdas and Gilham, 2004). In addition to the definition of the external contours, the definition of the computational domain has to include all the relevant details. For this type of problems, it will be enough to

include all the details greater than 0.5 m. The terrain details under this value will be considered part of its own roughness.

The main objective of this work is to determine the ideal localization of a new telescope for the solar observation in the Roque de los Muchachos Observatory (ORM) in the La Palma island, Spain. The starting point consists in assuming that the quality of the observation depends on the characteristics of the airflow pattern around the telescope building. Thus, it is necessary to know the site where the airflow is adequate for optimum observation. The best site can be guessed using Computational Fluid Dynamics simulations.

The results presented in this paper are part of the work carried out by CIMNE for the Instituto de Astrofísica de Canarias (IAC), the Spanish public company in charge of the solar telescope preliminary studies.

2. PHYSICAL MODEL

2.1 Governing equations

We present in this section the governing equations considered to model external incompressible airflows.

The state of the airflows under consideration is generally turbulent, the Reynolds number being of the order of 10^5 up to 10^7 , so that turbulence modeling is necessary. In the perspective of the solution of large scale problems, ensemble averaging (also called Reynolds averaging) is performed to filter the Navier-Stokes equations, that is, to decompose the flow vari-

ables into average and fluctuating components. This decomposition introduces a new term in the momentum equations called the Reynolds stress tensor involving the correlations between the fluctuating components. The Reynolds stress tensor is modeled by the Boussinesq approximation, introducing at its turn a new unknown, the eddy viscosity ν_t . The resulting system is called the RANS (Reynolds Averaged Navier-Stokes) equations and reads:

$$\frac{\partial \mathbf{u}}{\partial t} + (\mathbf{u} \cdot \nabla) \mathbf{u} - 2\nabla \cdot [(\nu + \nu_t) \varepsilon(\mathbf{u})] + \nabla p = \mathbf{0} \quad (1)$$

$$\nabla \cdot \mathbf{u} = 0$$

where \mathbf{u} and p are the unknowns of the problem, that is the velocity and pressure; ρ and ν are the air density and kinematic viscosity and $\varepsilon(\mathbf{u})$ is the velocity strain rate tensor, defined as:

$$\varepsilon(\mathbf{u}) = \frac{1}{2} (\nabla \mathbf{u} + \nabla \mathbf{u}^t)$$

While the two-equation k - ε turbulence model is extensively used in the simulation of external flows, a more simple one-equation turbulence model, namely the Spalart-Allmaras (SA) model (Spalart and Allmaras, 1992), was preferred for several reasons: it involves only one additional differential equation; it is computationally robust; in forced convection situations it gives similar results to two-equation turbulence models. The Spalart-Allmaras turbulence model consists of a single partial differential transport equation that solves for the eddy viscosity such that:

$$\frac{\partial \nu_t}{\partial t} + \mathbf{u} \cdot \nabla \nu_t + c_{w1} f_w \frac{\nu_t^2}{d^2} \quad (2)$$

$$- \frac{1}{\sigma} \nabla \cdot [(\nu + \nu_t) \nabla \nu_t] = \frac{c_{b2}}{\sigma} (\nabla \nu_t)^2 + c_{b1} S \nu_t$$

where c_{w1} , σ , c_{b1} and c_{b2} are constants of the model, S is the module of the vorticity, d is the distance to the wall and f_w is a function of the vorticity, the distance to the wall, and the eddy viscosity itself. The version displayed here holds for high-Reynolds number flows. A low-Reynolds number version, which includes additional terms, is also available. It is not shown here for the sake of clarity.

2.2 Boundary conditions

The following boundary conditions are considered in this work

$$\begin{aligned} \mathbf{u} &= \mathbf{u}_\infty, \quad \nu_t = \nu_{t\infty} \text{ at inflow,} \\ \mathbf{u} \cdot \mathbf{n} &= 0, \quad \boldsymbol{\sigma} \cdot \mathbf{n} - (\mathbf{n} \cdot \boldsymbol{\sigma} \cdot \mathbf{n}) \mathbf{n} = \mathbf{t}_y, \\ \nu_t &= \nu_{t,y} \text{ on walls,} \\ \boldsymbol{\sigma} \cdot \mathbf{n} &= \mathbf{0}, \quad \nabla \nu_t \cdot \mathbf{n} = \mathbf{0} \text{ at outflow.} \end{aligned} \quad (3)$$

Although the Spalart-Allmaras turbulence model takes into account near-wall (viscous) effects, the RANS equations are rarely integrated up to the wall, where the exact boundary conditions are $\mathbf{u}=\mathbf{0}$ and $\nu_t=0$. In fact, the only way to capture the sharp gradients inside the boundary layer is to use a very fine mesh, a solution which can be prohibitive for high Reynolds number flows and the large domains in play in the present problems. The strategy adopted here is based on the law of the wall. By assuming that the computational domain is located inside the boundary layer at a distance y from the real wall, the law of the wall enables one to calculate the tangential component of the traction \mathbf{t}_y and the eddy viscosity ν_t at y . The law of the wall first assumes that there exists a velocity scale in the boundary layer, called the friction velocity U_* , which is a function of the wall shear stress τ_w such that:

$$U_* = \sqrt{\tau_w / \rho} \quad (4)$$

It then states that the flow is parallel to the wall with velocity u such that:

$$u^+ = f(y^+) \quad (5)$$

with $u^+ = u/U_*$, and where $y^+ = yU_*/\nu$ is the dimensionless distance to the wall. Here, $f(y^+)$ is given by Reichardt's law, which mimics the zero pressure boundary layer flow:

$$\begin{aligned} f(y^+) &= \frac{1}{\kappa} \ln(1 + 0.4y^+) \\ &+ 7.8 \left[1 - e^{-y^+/11} - \frac{y^+}{11} e^{-0.33y^+} \right] \end{aligned} \quad (6)$$

Assuming that the shear stress is constant across the boundary layer ($|\mathbf{t}_y| = \tau_w$), and that it is directed to the opposite direction of the flow, we have therefore that inside the boundary layer

and *a fortiori* at y

$$\mathbf{t}_y = -\rho U_*^2 \frac{\mathbf{u}}{|\mathbf{u}|} \quad (7)$$

Figure 1 illustrates the algorithm.

For the eddy viscosity, the following law of the wall is used (Houzeaux and Codina, 2003):

$$\nu_{ty} = \nu \kappa^2 (y^+)^2 \left[1 - e^{-y^+/26} \right]^2 \frac{du^+}{dy^+} \quad (8)$$

Of course, this procedure is iterative, as the velocity \mathbf{u} is unknown when updating the tangential traction and the eddy viscosity. The global algorithm consists in the following:

1. Set initial conditions for \mathbf{u} and ν_{ty} . Set y .
2. Compute U_* using Eq. (5) and (6) with $u=|\mathbf{u}|$.
3. Impose \mathbf{t}_y using Eq. (7).
4. Compute ν_{ty} using Eq. (8).
5. Solve the RANS (1) and SA (2) equations.
6. If convergence not achieved, go to 2.

3. NUMERICAL MODEL

The set of partial differential equations is solved using the finite element method. We will not give any detail concerning the precise numerical model used in this work but only mention the most important points.

The time integration uses either the backward Euler or the Crank-Nicholson schemes. Both are unconditionally stable. The former is of first order while the latter is of second order.

Once the variational problems have been established, the next step is to undertake the finite element approximations to them. It is also necessary to use a stabilization method capable of dealing with all the instabilities that the standard Galerkin method presents. For the particular case of the Navier-Stokes equations it includes the pressure instability (equal order interpola-

$$\mathbf{u} \text{ known} \Leftrightarrow U_* \text{ (wall law)} \Leftrightarrow \mathbf{t}_y = -\rho U_*^2 \mathbf{u} / |\mathbf{u}|$$

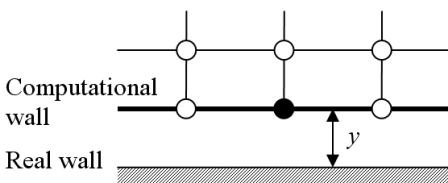


Figure 1: Impose the law of the wall on ●.

tion is used) and the instability arising in convection-dominated situations. The stabilization technique used here is the Algebraic Subgrid Scale model (ASGS) of (Codina, 2001) and originally proposed in (Hugues, 1995).

4. SIMULATION

4.1 Geometrical aspects

It is usually stated that the most time consuming step of a CFD simulation is the pre-process, that is, the geometry construction and the meshing of the computational domain. This was definitely the case in the present work. A 3D surface of about 100 km² was generated from the contour lines, 10 telescope buildings were drawn and six different meshes were generated.

Two computational domains were considered to solve the airflow around the telescope facilities. The first was a very large region with a relatively coarse mesh. The aerodynamic analysis with this mesh was performed to obtain the qualitative flow pattern of the region surrounding the telescope. The second was a region in the neighborhood of the new telescope with a mesh finer than the former. In the following sections we describe in more detail these two analyses.

4.2 Analysis of the large region

Due to the fact that the wind information near the telescope facilities was unknown, the analysis to obtain the flow pattern of a large region surrounding the telescope was carried out. This preliminary analysis was used to determine the boundary conditions for the accurate calculation of the flow around the building, assuming that the flow far from the telescope is unaffected by it.

The discretized domain of La Palma island was a section of 10 x 7.6 km with an average height of 1,400 m so the total surface was about 100 km². The main wind velocities (1 and 4 m/s) and directions (North, East and West), obtained from an experimental weather database, were prescribed.

The generated mesh for this domain was formed by 92,000 tetrahedral elements. The generated surface mesh is shown in Figure 2. This coarse mesh was used to obtain a stationary solution of the flow. We knew in advance

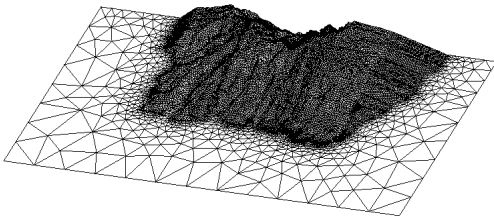


Figure 2: Generated surface mesh of the large region.

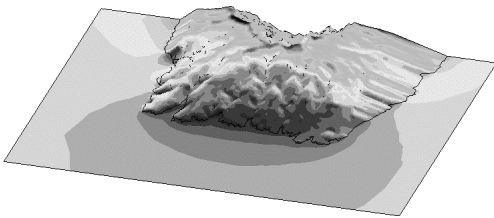


Figure 3: Pressure distribution.

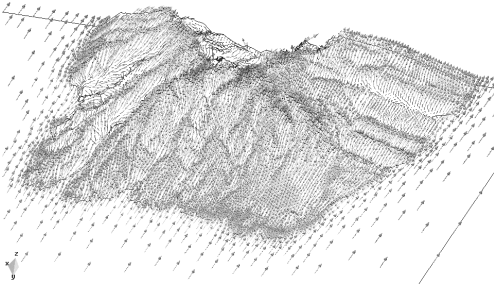


Figure 4: Velocity vectors.

that using this mesh it is impossible to capture all the details of the flow. Even though the oscillations of the flow were not captured in the solution, the velocity field obtained was interpolated to use it as boundary condition of the following analysis.

Two samples of the obtained results are shown in Figures 3-4. These figures display the pressure distribution and the velocity vectors over the discretized surface of La Palma island for a North wind of 1m/s.

4.3 Analysis of the region surrounding the telescope building

This discretized domain was a spherical section of 683,000m² with an average height of 460m

and the generated mesh was composed of 150,000 tetrahedral elements. A general view of the discretized domain is shown in Figure 5.

The solution obtained with this finer mesh is not stationary as in the previous region simulated. In the computed flow pattern, multiple vortex shedding and flow separation were observed. The results presented in this paper correspond to a wind velocity of 1m/s from the North direction and have been carried out to the second possible location of the new telescope.

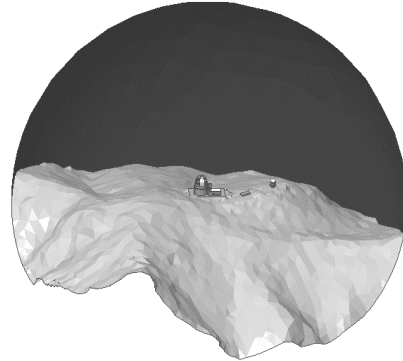


Figure 5: Discretized domain, where the new solar telescope, an optical telescope and an assistant building are included.

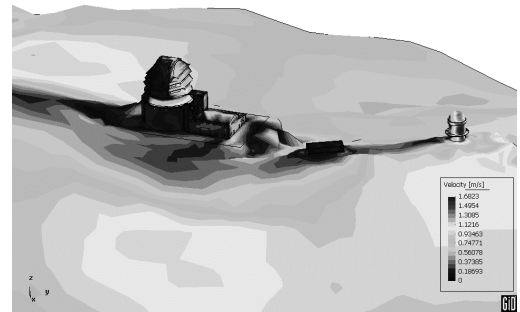


Figure 6: Velocity field.

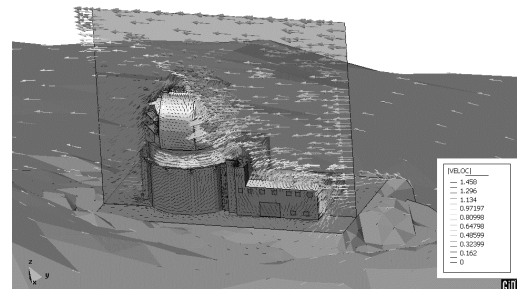


Figure 7: Detail of the velocity vectors around the telescope.

These results are summarized in Figures 6-7.

From the design point of view, these simulations must help to decide which location is the best to place the telescope building.

Spalart, P.R. and S.R. Allmaras, 1992. A One-equation Turbulence Model for Aerodynamic Flows. AIAA Paper 92-0439.

5. CONCLUSIONS

In this paper a methodology to simulate large buildings has been presented. In particular, this methodology has been applied to a singular telescope building, where the main goal was to define its correct location.

This study was divided in two stages. Within the first, an external aerodynamic analysis of a large region around the telescope facilities was carried out. This analysis was necessary due to the lack of experimental wind velocity data in the region surrounding the building, so the main goal of this part was to obtain the velocity field. The velocity outputs of this first analysis were applied as boundary conditions for the flow analysis in the neighborhood region of the building telescope, within the second part of the study. By following this procedure, we were able to define an air flow pattern in a concrete zone starting from a weather data distant of the studied zone.

The second analysis aimed to obtain the flow around the telescope, which gives an indication of possible visibility problems caused by the movement of particles that the air can do or variations in the density of the air. The analysis of these visibility problems in the selected sites will help the promoters to choose the best place where the new telescope might be erected.

REFERENCES

- Codina, R., 2001. A stabilized finite element method for generalized stationary incompressible flows. *Computer Methods in Applied Mechanics and Engineering*, 190(20-21), pp. 2681-2706.
- Houzeaux, G. and R. Codina, 2003. A Dirichlet/Neumann domain decomposition method for incompressible turbulent flows on overlapping subdomains, *Comput. Fluids*, Vol. 33, No. 5-6, pp. 771-782.
- Hughes, T.J.R., 1995. Multiscale Phenomena: Green's functions, the Dirichlet-to-Neumann formulation, sub-grid scale models, bubbles and the origins of stabilized methods, *Computer Methods in Applied Mechanics and Engineering*, Vol. 127, pp. 387-401.
- Scaperdas, A. and S. Gilham, 2004. Thematic Area 4: Best practice advice for civil construction and HVAC, *The QNET-CFD*, Vol. 2, No. 4, pp. 28-33.